J Electroceram (2009) 23:502–505
DOI 10.1007/s10832-008-9519-x

# Synthesis and piezoelectric properties of $(1-x)(Na_{0.5}K_{0.5})NbO_3$–$x(Ba_{0.95}Sr_{0.05})TiO_3$ ceramics

**Mi-Ro Kim · Hyun-Cheol Song · Ji-Won Choi · Yong-Soo Cho · Hyun-Jai Kim · Seok-Jin Yoon**

Received: 3 June 2007 / Accepted: 25 April 2008 / Published online: 28 June 2008


**Abstract** $(1-x)(Na_{0.5}K_{0.5})NbO_3$–$x(Ba_{0.95}Sr_{0.05})TiO_3$ [$(1-x)$NKN–$x$BST] ceramics were synthesized by the conventional solid-state sintering, and their microstructure and piezoelectric properties were investigated. The sintering temperature of the specimens was 1075 °C in air atmosphere and a morphotropic phase boundary (MPB) was observed in the specimens with $0.03 \leq x \leq 0.05$. Compared with the piezoelectric properties of the NKN ceramics, the enhanced $d_{33}$ value of 136 pC/N and $\varepsilon_3^T/\varepsilon_o$ value of 671 were obtained for the $(1-x)$NKN–$x$BST specimens with $x = 0.03$.

**Keywords** Piezoelectric properties · Lead-free · $(Na_{0.5}K_{0.5})NbO_3$ · Perovskite structure

## 1 Introduction

In application of electronic devices such as actuators, transducers, sensors, and filters, the $Pb(Zr_{1-x}Ti_x)O_3$ (PZT) ceramics have been widely used due to their excellent piezoelectric properties [1–4]. Nevertheless, they contain more than 60 wt% of PbO, which can give rise to serious environmental pollution. To solve this problem, recent studies were focused on Pb-free piezoelectric materials and $(Na_{0.5}K_{0.5})NbO_3$ (NKN) ceramics, especially, have aroused attention as a substitute for PZT ceramics because of their high curie temperature and excellent piezoelectric characteristics [5–7]. NKN has piezoelectric properties of $d_{33} \approx$ 80~100pC/N, $k_p \sim 34$, $Q_m \sim 130$ and $T_c \sim 420$°C [8]. However, potassium in NKN ceramics is likely to volatilize rapidly at around the sintering temperature over 1140°C, and have difficulty in achieving high density NKN ceramics resulted from the tendency of absorbing vapor in the atmosphere during the manufacturing process [9–13]. To avoid these problems, $(1-x)$NKN–$x$PbTiO$_3$, $(1-x)$NKN–$x$LiTaO$_3$ and $(1-x)$KNbO$_3$–$x$LaFeO$_3$ solid solutions were investigated [14–16]. Recently, $(1-x)$NKN–$x$SrTiO$_3$, $(1-x)$NKN–$x$BaTiO$_3$ ceramics were studied and were found to exhibit good piezoelectric properties [17–19].

$BaTiO_3$ is a ferroelectric material, which shows high dielectric and piezoelectric constant. $SrTiO_3$ is a paraelectric material, which shows low dielectric loss.

In this work, $(Ba_{0.95}Ti_{0.05})O_3$ ceramics were added to NKN ceramics to improve the piezoelectric properties of NKN due to adding ferroelectric compound and the experiment were designed to consider how the changes in compositions and amount of BST additives would affect the piezoelectric properties of NKN ceramics.

## 2 Experimental procedure

$(1-x)(Na_{0.5}K_{0.5})NbO_3$–$x(Ba_{0.95}Sr_{0.05})TiO_3$ ceramics ($x$ = 0, 0.03, 0.05, and 0.07) were prepared by the conventional solid-state reaction method. The starting materials were $K_2CO_3$ (99 %, Aldrich), $Na_2CO_3$(99.5 %, Aldrich), $Nb_2O_5$(99.9 %, Aldrich), $BaCO_3$(99 %, Aldrich), $SrCO_3$(99.9 %, Aldrich), and $TiO_2$(99.8 %, Aldrich). They were ball-milled in a polyethylene jar with $ZrO_2$ balls and anhydrous ethanol for 24 h. After drying, they were calcined at 950 °C for 2 h. The calcined powders were ball-milled again for 72 h and then dried, and sifted through a

M.-R. Kim · H.-C. Song · J.-W. Choi (✉) · H.-J. Kim · S.-J. Yoon
Thin Film Materials Research Center, KIST,
Seoul, Korea
e-mail: jwchoi@kist.re.kr

M.-R. Kim · Y.-S. Cho
Department of Ceramic Engineering, Yonsei University,
Seoul, Korea

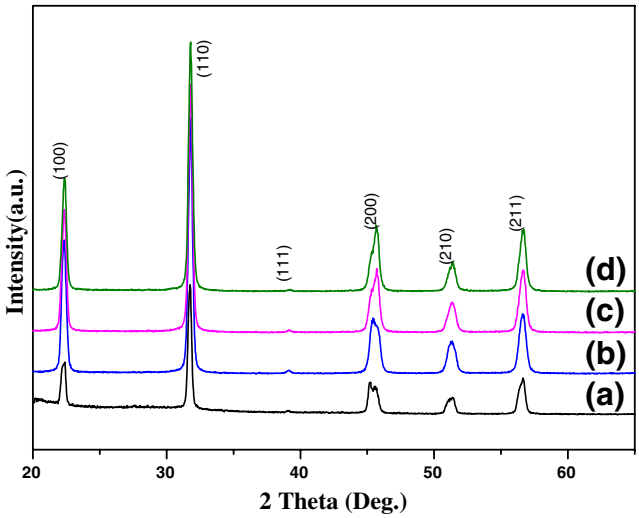


**Fig. 1** XRD Pattern of the (1−*x*)NKN–*x*BST ceramics: (**a**) pure NKN, (**b**) $x$=0.03, (**c**) $x$=0.05, and (**d**) $x$=0.07

150 mesh sieve. The powders were pressed uni-axially into the disk shape of 18 mm diameter under 100 MPa. The green bodies were sintered in air at 1075 °C for 2 h. Silver paste was coated on both sides of the samples and fired at 650 °C for 15 min as electrodes for measurement of the dielectric and piezoelectric properties. The crystal structure was determined by x-ray diffraction analysis (XRD; DY 983, Philips, Netherlands), and the microstructure of the sample was observed by scanning electron microscopy (SEM; S-3000H, Hitachi, Japan). Their dielectric properties were measured using Agilent 4294A precision impedance analyzer at the room temperature. For piezoelectric and electromechanical measurements, the samples were poled in silicone oil at 120 °C by applying a dc field of 4 kV/mm for 60 min. The piezoelectric constant ($d_{33}$) and the electromechanical coupling coefficients ($k_p$) were measured using a piezo $d_{33}$ meter (Channel Product DT-3300) and impedance analyzer (Agilent 4294A) respectively.

## 3 Results and discussion

Figure 1 shows the XRD patterns of (1 − $x$)NKN–$x$BST ceramics sintered at 1075°C for 2 h. It was found that the (1 − $x$)NKN–$x$BST ceramics formed the orthorhombic structure in the case of $x \leq 0.03$. As increasing of the amount of BST composition, the structure was changed, and when the amount was $0.03 \leq x \leq 0.05$, morphotropic phase boundary (MPB) coexisting orthorhombic and tetragonal phases was observed. The amount was $x > 0.05$, the crystal symmetry exhibited a small tetragonal distortion. According to the Fig. 1, the only peaks for perovskite structure were observed. Hence, the BST ceramics which also have the perovskite phase seemed to form a solid solution with NKN ceramics in which Ba and Sr ions occupied Na and K ion sites and Ti ions entered Nb ion sites of NKN [20].

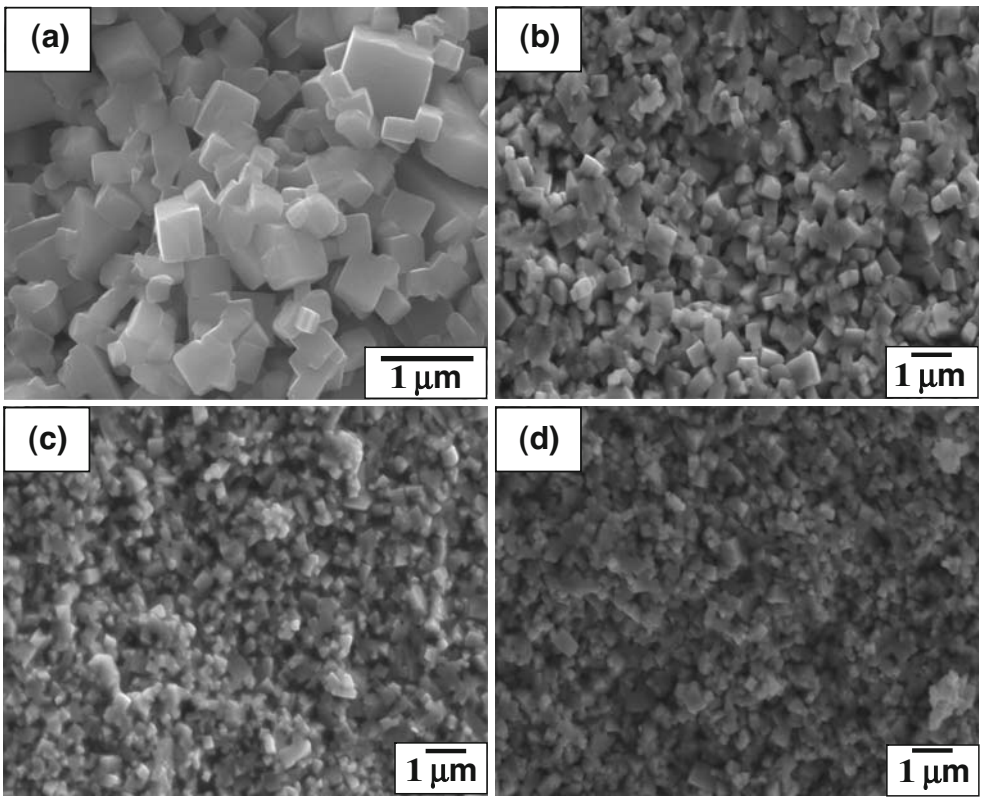


**Fig. 2** SEM images of the (1−*x*)NKN–*x*BST ceramics: (**a**) pure NKN, (**b**) $x$=0.03, (**c**) $x$=0.05, and (**d**) $x$=0.07

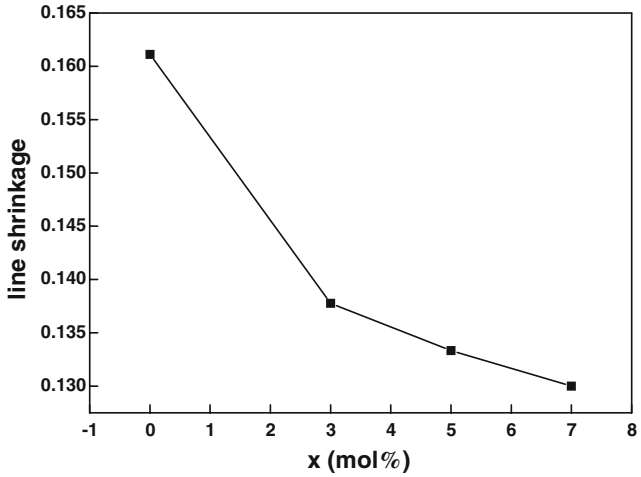


**Fig. 3** Line shrinkage of $(1-x)$NKN–$x$BST ceramics as a function of the BST content $x$

Figure 2 illustrates microstructure of $(1-x)$NKN–$x$BST ceramics sintered at 1075 °C for 2 h. It could be seen that the pure NKN ceramics were consisted of very large and dense grains compared with other specimens. However, as increasing of BST content, the grain size became small, due to the low sinterability of BST at relatively low sintering temperature of 1075 °C [21, 22].

Figure 3 exhibits the line shrinkage of $(1-x)$NKN–$x$BST ceramics sintered at 1075 °C for 2 h.

$$\text{shrinkage} = \frac{(\text{Sample diameter before sintering}) - (\text{Sample diameter after sintering})}{\text{Sample diameter before sintering}} \times 100$$

It was found that the line shrinkage decreased with the BST addition. Based on this result, sinterability of $(1-x)$NKN was declined as the amount of BST was increased which may be attributed to high sintering temperature of BST ceramics.

Figure 4 shows the dielectric constant ($\varepsilon_3{}^T/\varepsilon_o$) and the piezoelectric constant ($d_{33}$) of $(1-x)$NKN–$x$BST ceramics sintered at 1075 °C for 2 h. The dielectric constant was elevated with the addition of BST ceramics and this could be possible because BST ceramics are well-known ferroelectric materials which exhibit high $\varepsilon_3{}^T/\varepsilon_o$ values. Therefore, BST ceramics seemed to play a role to increase $\varepsilon_3{}^T/\varepsilon_o$. The $d_{33}$ value reached its maximum value of 136 pC/N when 3 mol% of BST was added, and decreased as further addition of BST ceramics. Since MPB region appeared when BST amount was $0.03 \le x \le 0.05$, as shown in Fig. 1, the highest $d_{33}$ value at 3 mol% of BST could be accounted for the results.

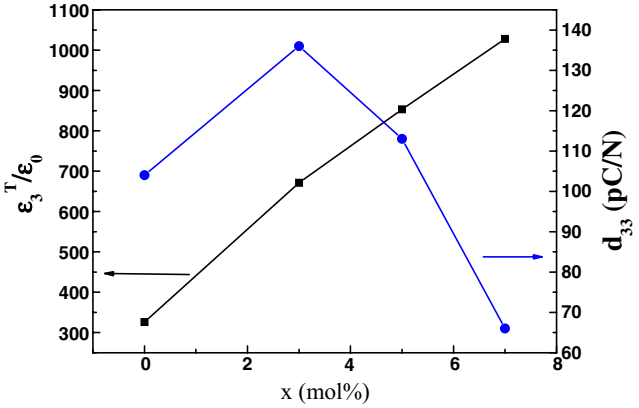


**Fig. 4** Dielectric constant and Piezoelectric constants of $(1-x)$NKN–$x$BST ceramics as a function of the BST content $x$

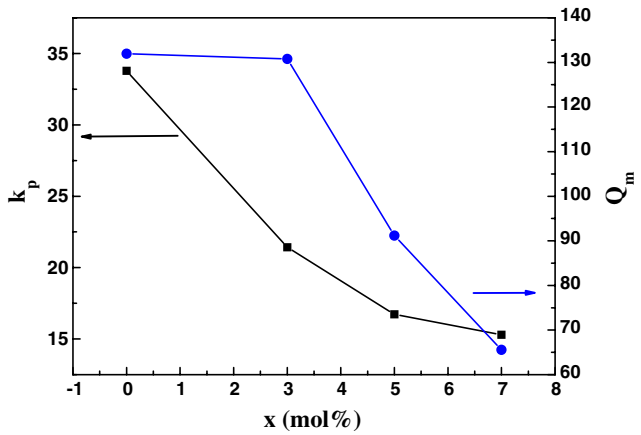


**Fig. 5** Electromechanical coupling and quality factors of $(1-x)$NKN–$x$BST ceramics as a function of the BST content $x$

Figure 5 illustrates the electromechanical coupling factors ($k_p$) and quality factors ($Q_m$) of $(1-x)$NKN–$x$BST. As increasing the amount of BST composition, the $k_p$ and $Q_m$ values are decreased. According to the Figs. 2 and 3, the grain size and linear shrinkage were small and low, respectively. In general, since a grain boundary is a three dimensional defect, existence of grain boundary could deteriorate the $Q_m$ value. The $k_p$ value was also reported to have correlation with the specimen density. Thus, as well as the low sinterability, high grain boundary density in $(1-x)$NKN–$x$BST ceramics when $x$ amount increased may

**Table 1** Electrical properties of NKN and 0.97NKN-0.03BST ceramics.

| Composition | $d_{33}$ (pC/N) | $k_p$ (%) | tan$\delta$ | $Q_m$ |
|---|---|---|---|---|
| NKN | 104 | 33.78 | 0.02 | 131.95 |
| 0.97NKN-0.03BST | 136 | 21.43 | 0.08 | 130.76 |

result in low $Q_m$ and $k_p$ value of the ceramics. In Table 1, the comparison of piezoelectric properties for NKN and 0.97NKN-0.03BST ceramics were displayed. 0.97NKN-0.03BST ceramics showed a highly improved $d_{33}$ value comparing to NKN ceramics even though they have a lower $k_p$ and $Q_m$ value.

## 4 Conclusions

$(1 - x)$NKN–$x$BST system which has a high $d_{33}$ value was synthesized by solid-state reaction method. The results showed that the grain size of the BST decreases with increasing the amount of BST. A noticeable increase of permittivity was observed as an addition of BST ferroelectric material. But $k_p$ value was decreased with an addition of BST. The morphotropic phase boundary between orthorhombic and tetragonal phases is found at $0.03 \leq x \leq 0.05$ and $0.97(Na_{0.5}K_{0.5})NbO_3$–$0.03(Ba_{0.95}Sr_{0.05})TiO_3$ ceramics showed good piezoelectric properties of $\varepsilon_3^T/\varepsilon_o = 671$, $Q_m = 130.76$, $d_{33} = 136$ pC/N.

## References


1. B. Jaffe, W.R. Cook, H. Jaffe, *Piezoelectric ceramics* (Academic, New York, 1971)(chapter 8)
2. Y. Lu, D.Y. Jeong, Z.Y. Cheng, Q.M. Zhang, H.S. Luo, Z.W. Yin, D. Viehland, Appl. Phys. Lett. **78**, 3109 (2001)
3. W. Ren, S.F. Liu, B.K. Mukherjee, Appl. Phys. Lett. **80**, 3174 (2002)
4. S.E. Park, T.R. Shrout, J. Appl. Phys. **82**, 804 (1997)
5. E. Ringgaard, T. Wurlitzer, J. Eur. Ceram. Soc. **25**, 2701 (2005)
6. H. Du, Z. Li, F. Tang, S. Qu, Z. Pei, W. Zhou, Mater. Sci. Eng. B **131**, 83 (2006)
7. S.H. Park, C.W. Ahn, S. Nahm, J.S. Song, Jap. J. Appl. Phys. **43**, L1072 (2004)
8. T.R. Shorut, S.J. Zhang, J. Electroceram. **19**, 111 (2007)
9. R.C. Zhou, Y.X. Liu, X.M. Meng, J. Electroceram. **18**, 9 (2007)
10. W. Chen, Y. Li, Q. Xu, J. Zhou, J. Electroceram. **15**, 229 (2005)
11. B.P. Zhang, J.F. Li, K. Wang, H. Zhang, J. Am. Ceram. Soc. **89**, 1605 (2006)
12. J.F. Li, K. Wang, J. Am. Ceram. Soc. **89**, 706 (2006)
13. R. Zuo, J. Rödel, J. Am. Ceram. Soc. **86**, 2010 (2006)
14. Y. Guo, K.I. Kakimoto, H. Ohsato, Mater. Lett. **59**, 241 (2005)
15. R. Wang, R. Xie, T. Sekiya, Y. Shimojo, Jpn. J. Appl. Phys. **41**, 7119 (2002)
16. K. Kakimoto, I. Masuda, H. Ohsato, Jpn. J. Appl. Phys **42**, 6102 (2003)
17. C.W. Ahn, H.C. Song, S. Nahm, S.H. Park, K. Uchino, S. Priya, H.G. Lee, N.K. Kang, Jpn. J. Appl. Phys, **44**, L1361 (2005)
18. H.Y. Park, C.W. Ahn, H.C. Song, J.H. Lee, S. Nahm, K. Uchino, H.G. Lee, H.J. Lee, Appl. Phys. Lett. **89**, 062906 (2006)
19. V. Bobnar, J. Bernard, M. Kosec, Appl. Phys. Lett. **85**, 994 (2004)
20. Y. Guo, K.I. Kakimoto, H. Ohsato, Jpn. J. Appl. Phys. Part 1 **43**, 6662 (2004)
21. A. Loachim, M.I. Toacsan, M.G. Banciu, G. Stoica, H.V. Alexandru, Thin Solid Films **515**, 6289 (2007)
22. H. Reisinger, H. Wendt, G. Geitel, E. Fritsch, Symposium on VLSI Technology **1998**, 58 (1998)